Published in final edited form as:
Science. 1992 April 10; 256(5054): 198–203.

Lambda Int Protein Bridges Between Higher Order Complexes at Two Distant Chromosomal Loci *att*L and *att*R

Sunghoon Kim[*] and **Arthur Landy**[†]
The authors are in the Division of Biology and Medicine, Brown University, Providence, RI 02912.

Abstract

The excisive recombination reaction of bacteriophage lambda involves a specific and efficient juxtaposition of two distant higher order protein-DNA complexes on the chromosome of *Escherichia coli*. These complexes, which mediate synapsis and strand exchange, consist of two DNA sequences, *att*L and *att*R, the bivalent DNA binding protein Int, and the sequence-specific DNA bending proteins, IHF, Xis, and Fis. The protein-protein and protein-DNA interactions within, and between, these complexes were studied by various biochemical techniques and the patterns of synergism among pairs of mutants with marginally impaired recombination function were analyzed. The DNA bending proteins facilitated long-range tethering of high- and low-affinity DNA sites by the bivalent Int protein, and a specific map is proposed for the resulting Int bridges. These structural motifs provide a basis for postulating the mechanisms of site-specific recombination and may also be relevant to other pathways in which two distant chromosomal sites become associated.

Higher order protein-DNA structures are central features in the initiation of DNA replication, the regulation of transcription, and many pathways of site-specific recombination (1). Although these reactions may differ chemically, they all have a high degree of specificity and complex regulatory elements. One example of such higher order structures is the site-specific recombination pathway of bacteriophage lambda. We now present data and suggest a model for a synaptic complex, in which 270 base pairs (bp) of DNA containing 15 protein binding sites interact with four different proteins to make a recombinogenic structure, that includes two chromosomal sites separated by more than 40,000 bp (40 kb).

Excision of bacteriophage lambda DNA from its *Escherichia coli* host chromosome depends on site-specific recombination between two specific DNA sequences called prophage *att* sites (*att*L and *att*R). The products of this recombination, *att*P on the excised phage chromosome and *att*B on the bacterial chromosome, are themselves substrates for the integrative recombination that generated the integrated provirus (2,3). During recombination, strand exchange is executed by the phage-encoded protein, integrase (Int), which is a type I topoisomerase with DNA nicking and closing activity (4,5). Int has two autonomous DNA binding domains, and each recognizes different DNA sequences: (i) the amino-terminal domain binds with high affinity to “arm-type” sites distant from the region of strand exchange; and (ii) the carboxyl-terminal domain, which also contains the DNA nicking activity, binds with low affinity to “core-type” sites at the loci of strand exchange (6–8).

Three accessory proteins involved in the recombination reaction, IHF, Xis, and Fis, all bind specific sequences and induce dramatic DNA bends (9–14). IHF is required for both integrative and excisive recombinations whereas Xis stimulates only the latter (15,16). When Xis is limiting, as is the case in vivo, Fis substitutes for one of the two Xis protomers (13,17). The

†To whom all correspondence should be addressed.
*Present address: Department of Biology, Massachusetts Institute of Technology, Cambridge, MA 02139.

sites for these DNA bending proteins are located between the arm- and core-type Int binding sites (Fig. 1). This arrangement of binding sites has been explained by the finding that an IHF-induced bend in *att*L delivers Int bound at a distal high-affinity arm-type site to a low-affinity core-type site (18). The structural role of IHF was confirmed by demonstrating that one IHF binding site can be replaced either by the intrinsic curvature of phased A-tract DNA or by another DNA bending protein (19). Although Fis was not used in the studies described below, the Xis-Fis pair is functionally equivalent to the Xis-Xis pair in every aspect of the lambda (λ) recombination pathway that has been tested (9,13,17).

Together, these proteins form specific higher order complexes with *att* DNA. Their formation is optimized by supercoiling and sequence-determined intrinsic curvature (20–24), which are DNA properties, and by cooperative interactions among the proteins that bind at adjacent and well-separated sites on the *att* DNA (18,24–26). The protein-protein and protein-DNA interactions mediated by IHF-induced DNA bending have been mapped in *att*L, and a model for this *att*L higher order structure has been proposed (26). Insights regarding the nature of the interactions between recombinogenic partners also comes from the findings (i) that *att*B does not appear to acquire Int from solution, but rather from a preformed *att*P complex and (ii) that *att*L complexes enhance Int cleavage and strand transfer at the core of *att*R (27–29). Although excision of a prophage from the host chromosome is an intramolecular reaction between two distant *att* sites, in this article we refer to interactions between *att*L and *att*R complexes as "intermolecular" since this reflects the most common experimental conditions.

Enhancement of Int binding at the low-affinity core sites of *att*R

The *att*R junction contains a complex array of protein binding sites that are apportioned between the DNA bending proteins (IHF, Xis, and Fis) and the NH_2- and COOH-terminal domains of Int (Fig. 1). Although we have already described the interactions of Int protein at the high-affinity arm-type binding sites of *att*R, we have not addressed the binding of Int at the low-affinity core-type sites, where strand exchange occurs. One sensitive and functionally relevant assay of Int binding at the core-type sites is afforded by suicide substrates that were designed to trap the high-energy covalent Int-DNA intermediates generated when Int cleaves DNA at the sites of strand exchange (Fig. 2, top) (18,26,30). With normal recombination substrates, these covalent intermediates are transient and difficult to detect in that the phosphodiester bond between the active site tyrosine of Int and the 3′ end of the cleaved strand is rapidly attacked by a nearby 5′ hydroxyl, thus restoring the original cleavage site or creating a new junction with a strand from the recombination partner (28). This ligation step is blocked in the *att* suicide substrates, which contain a preexisting nick within the overlap region several bases away from the Int cleavage site. When this nicked *att* site is cleaved by Int, a small oligonucleotide is generated. Diffusion of the oligonucleotide removes the 5′-OH nucleophile, thereby trapping the otherwise transient covalent bond between Int and the cleaved DNA strand. As shown earlier, the amount of Int delivered productively to the suicide core site is monitored as the amount of covalent Int-DNA complex accumulated during the reaction (18, 26,30). Under the conditions used in our experiments, top- and bottom-strand nicked substrates provided a measure of Int cleavage at the core sites for top-and bottom-strand exchange, respectively (Fig. 2, top). The *att*R suicide substrates with a nick either in the top or bottom strand were incubated with Int in the presence or absence of IHF and Xis, and the effect of these proteins on Int cleavage at the two core sites was examined. Although IHF and Xis together stimulated Int cleavage at the core sites, neither protein alone had much effect (Fig. 2, bottom).

In excisive recombination, the leftmost Int and IHF sites of *att*R (P1 and H1) are not required (24,31,32), and the core site for bottom-strand exchange (B′) is not required through synapsis and the first strand exchange (28). These observations simplify the analysis of the role of the

P2 Int binding site and make it possible to use an *att*R suicide substrate that lacks DNA to the right of the overlap region. In such a "half-*att*R" substrate, the top-strand core site (C) is located a few base pairs from the end of the fragment. Int cleavage at the C site generates a small diffusible oligonucleotide that traps the covalent intermediate in a manner similar to a top-strand nicked substrate (18,26,28). These substrates also lack the superfluous P1 and H1 sites, and thus correspond to the minimal *att*R recombination partner.

When the minimal half-*att*R was incubated with Int under the conditions used to assay formation of the covalent complex, there was efficient Int cleavage at the core site, and this cleavage depended on the presence of IHF and Xis (Fig. 3, left). Complex formation was abolished by deletion of the P2 Int binding site (Fig. 3, left) or by inactivating the P2 site with multiple base substitutions (33). These results suggest that the stimulation observed with IHF and Xis requires the P2 site.

To establish the relevance of these assays to the recombination pathway, we monitored the ability of the minimal half-*att*R substrate to undergo synapsis with *att*L and to execute top-strand transfer. The nonspecific carrier DNA in the cleavage assays was replaced by homologous *att*L recombination partner, and top-strand transfer was measured in the presence of Int, IHF, and Xis. As was expected, the minimal half-*att*R substrate was an efficient strand transfer partner and this reaction also depended on the P2 site (Fig. 3, right), an indication that the observed P2-IHF-Xis-dependent Int binding (cleavage) at the core site does correspond to an early step in excisive recombination.

Higher order structure of the *att*R complex

There are two classes of models for the P2 enhancement of Int cleavage at the *att*R core sites. In the first model, DNA bending by IHF and Xis mediates direct delivery of Int from the P2 site to one of the core sites; the same Int molecule binds to P2 with its NH_2-terminal domain and to a core site with its COOH-terminal domain. At the second core site an Int is recruited from solution and its binding is likely to be facilitated by protein-protein interactions. According to this model, there would be two Int molecules in the *att*R complex: one doubly bound at P2 and the corresponding core site and one singly bound at the other core site. In the second model, the Int bound at P2 does not itself bind to the *att*R core sites; rather, two additional Int molecules are recruited from solution and stabilized at the two core sites by protein-protein interactions. In this model, the *att*R complex would contain three Int molecules, each of which is singly bound to its respective site.

These two models were tested in a gel mobility shift assay with a minimal *att*R (lacking the P1 and H1 sites) that monitored the formation of Int-IHF-Xis-*att*R complexes (Fig. 4). The DNA bending induced by IHF binding at H1, or Xis binding at X1 and X2, resulted in complexes with greatly retarded gel mobility (labeled RH and RX, respectively) (9,11,12,31). When IHF and Xis simultaneously bound *att*R DNA, the mobility of the complex (RHX) was more retarded than with either protein alone. Addition of Int to RHX produced three new major bands, labeled RHX1-RHX3 in order of decreasing gel mobility. The transition from the faster- to the slower-moving complexes occurred with increasing amounts of Int in the same range that produced increasing recombination efficiencies, and formation of RHX3 was abolished by deletion of the B′ core site (33). These results suggest that complexes RHX1–RHX3 resulted from the sequential binding of Int.

Immunoblotting of Int, when used to determine the relative number of Int molecules in each complex, confirmed that the ratios of Int to DNA in complexes RHX1–3 are 1:2:3. The relative ratios of Int to DNA were normalized to a ratio of 2 for complex RHX2 because this complex was produced over the entire range of Int concentrations used in these experiments. In four different experiments, the relative ratios of Int to DNA (average ± SD) was 0.9 ± 0.4 for

complex RHX1 and 3.0 ± 0.6 for complex RHX3 (34). These results support the second model; that is, within the IHF-Xis-Int-*att*R higher order complex, the P2-bound Int does not interact directly with the *att*R core sites, but instead facilitates the binding of other Int molecules at the core sites via protein-protein interactions.

Functional linkages between arm and core sites during recombination

There are three unsatisfied DNA binding domains in the proposed *att*R higher order structure. Specifically, the P2-bound Int has a free COOH-terminal domain that is available to bind a core-type site, and the core-bound Ints each have an NH_2-terminal domain that is available to bind arm-type sites. Each of these unsatisfied DNA binding domains affords a potential source of inter-molecular (synaptic) interactions with the *att*L complex, which also has a set of unsatisfied DNA binding domains (26). The higher order structures now proposed for *att*R and previously for *att*L lead to specific predictions about the map of intermolecular Int bridges that comprise the *att*R-*att*L synaptic complex. One intermolecular Int bridge is predicted between the *att*R P2 arm site and a core site of *att*L, whereas another is predicted between the *att*L P′2 arm site and a core site of *att*R (see below).

To study the functionally critical Int interactions that comprise the unstable synaptic complex, we developed a genetic approach. Individual arm and core sites were altered by site-directed mutations, each of which depressed recombination only partially (Table 1). If each Int within the synaptic complex is held by one arm-type and one core-type binding site, its retention within the complex is likely to be relatively resistant to small reductions in affinity at only one of its two binding sites. Reduced affinity at both binding sites of a particular Int is more likely to result in its loss from the synaptic complex. Therefore, a pair of arm and core mutations that affect binding of the same Int are likely to be synergistic; that is, they should depress recombination more than a pair of mutations affecting the arm site of one Int and the core site of another Int. Two conditions are necessary for this approach. First, mutations or reaction conditions must be such that each mutant site, by itself, produces only a modest impairment of recombination. Second, all possible pairwise combinations of mutant arm and core sites must be tested to ensure a self-consistent matrix of results. The first condition was satisfied by the appropriate choice of consensus sequence changes and reaction conditions (Table 1). The second condition was satisfied by the matrices of recombination crosses shown in Tables 2 to 4 and involving all of the arm-type sites required for excisive recombination (Fig. 1).

The P2 Int binding site was altered such that the recombination efficiency of this *att*R was approximately 25 percent less than that of a wild-type *att*R under these recombination conditions (Table 2, top row). The *att*R containing this impaired P2 site was then used in a series of four recombination reactions in which one core site at a time contained a mutation resulting in mild impairment of the reaction. Each of the four core site mutations was also tested in a recombination reaction with *att*R containing a wild-type P2 site. The combination of either core mutation in *att*R with the P2 arm mutation did not depress recombination efficiencies relative to the $P2^+$ *att*R (Table 2). However, the core mutations in *att*L were synergistic with the P2 arm mutation in *att*R. These results are consistent with the data presented above, suggesting that Int bound at the P2 arm site is held in the synaptic complex by an intermolecular bridge with a core site of *att*L. The observed depression of recombination with both *att*L core sites is consistent with previous results indicating that Int binding at the B core site is stabilized by protein-protein interactions with the Int bound at the C′ core site (7, 26).

In a similar experiment with the P′2 arm site of *att*L (Table 3), alteration of the consensus sequence reduced the recombination efficiency of the impaired *att*L approximately 15 percent relative to wild-type *att*L. Whereas the combination of the core mutations in *att*L with the P′2

arm mutation did not depress recombination efficiencies relative to the P′2$^+$ *att*L, the core mutations in *att*R were synergistic with the P′2 arm mutation in *att*L. Here also the results are consistent with the predictions, suggesting that the P′2 site of *att*L forms an intermolecular bridge with a core site of *att*R.

The analysis of the arm site mutants points to participation in intermolecular Int bridges for the P2 and P′2 sites. Although this result is consistent with the biochemical data, it is important to show that the intermolecular synergism is not an artifact of this experimental strategy. Fortunately, the third arm site involved in excisive recombination, P′1, affords a good control for this concern since it participates with the C′ core site in an intramolecular Int bridge that is particularly critical for the *att*L structure (26). Indeed, the same consensus sequence change used to impair the P′2 arm site has a greater effect on recombination when it is introduced into the P′1 site (Table 4, top row). Analysis of the combined effects of the P′1 arm mutation and each of the core site mutations show that the intramolecular combination with C′ produced the most severe inhibition of recombination, as predicted.

The relative patterns of pairwise synergism among all of the arm and core mutants remain the same when the recombination reactions are performed with different amounts of Int or at different salt concentrations (although the absolute levels of recombination may vary). Thus, the pair-wise effects of mutant arm and core Int binding sites on excisive recombination efficiency are consistent with all of the biochemical experiments and suggest that Int molecules bound at the P2 and P′2 arm-type sites participate in intermolecular bridges with their partners' core sites, while the Int bound at the P′1 arm site mediates an intramolecular bridge with the C′ core site. All of the genetic and biochemical results described above are consistent with previous findings: Int is held relatively weakly at the core sites of the *att*R complex (24,29); *att*L stimulates Int binding to the core sites of *att*R (28,29); Int bound to the P′2 site of *att*L has an unsatisfied COOH-terminal DNA binding domain; and P′1 and P′2 play a critical role in synapsis and the first strand exchange (26).

A model for synaptic interactions between *att*L and *att*R

The unsatisfied DNA binding domains of the Int proteins bound to *att*R, along with those in the previously studied *att*L structure (26), afford a potential bridging mechanism to promote synapsis. These bridges are most likely formed by monomeric Int, since Int is a monomer in solution and has also been shown to bind to *att* site DNA as a monomer (35–37). The intermolecular bridge formed by Int bound to the P2 arm site must be with the B site of *att*L since the other *att*L core site (C′) was previously shown to be involved in an intramolecular bridge with P′1 (26). The intermolecular bridge formed by Int bound to the P′2 arm site is most likely with the C site of *att*R, since the B′ site is not required for synapsis or top-strand exchange and the P′2 site and C sites are both required for these early steps of recombination (26,28). Accordingly, the B′ site would recruit an Int from solution; this is an Int that is not "delivered" by a high-affinity arm site and could even join the complex at a later stage of the reaction.

The basic motif of the proposed map of arm-core interactions (Fig. 5) is that protein-induced bends enable bivalent Int molecules to bridge appropriate pairs of high-and low-affinity sites. The path of the DNA and the relative orientations of *att*L and *att*R are not specifically addressed in this model and have been drawn to illustrate the proposed protein-DNA and protein-protein interactions of the bivalent Int protein. For clarity in a planar diagram, the *att*L and *att*R partners have been aligned in the most extreme version of the "antiparallel" orientation proposed by Stark *et al.* (38). There are several pathways by which the two partners could assemble. For instance, Int could bind the two DNAs without preference, or one partner that is devoid of Int could synapse with the Int-containing higher order complex of the other partner. It is also possible that the temporal order of some steps leading to synapsis is not precisely determined.

Since these particular experiments did not include Fis protein it is not shown in Fig. 5. However, numerous in vitro and in vivo experiments have shown that the Xis-Xis binding at X1X2 is functionally equivalent in every respect tested to Xis-Fis binding at X1-F (Fig. 1) (13,17).

Protein-protein interactions are also an important feature of the proposed map. In the *att*L complex, Int binding at one core site is stabilized by an Int bound at the other core site (7,26). This was reflected in the weak discrimination between B and C′ of *att*L and between C and B ′ of *att*R in the genetic test for synergism. Our results also indicate that the P2-bound Int of *att*R, which is delivered directly to the B site of *att*L in trans, facilitates the binding of additional Ints to its core sites in cis. Similarly, the P′2-bound Int of *att*L, which is delivered directly to the C site of *att*R in trans, also facilitates binding of another Int to its core sites in cis (26,28, 29).

Despite the reciprocality of shared Int bridges at synapsis there are significant differences between the *att*R and *att*L partners. In the *att*R complex, IHF-Xis-enhanced Int binding at the core sites did not give a strong signal in nuclease protection and heteroduplex cleavage assays (24,29) and could only be quantitated with the more sensitive suicide substrate assay. This contrasts with the *att*L complex, where IHF-dependent Int binding to the core sites in *att*L was not only observed by the suicide Int cleavage assay, but also by other methods (18,26,29). These differences imply that the *att*R complex promoted by IHF and Xis may be less stable than the *att*L complex induced with IHF alone. It is interesting that Xis, along with Int and IHF, does make a very stable complex with *att*P (25). Perhaps the relative instability of the *att*R complex facilitates its reactivity with *att*L, and the stability of the *att*P reaction product enhances the directionality of excisive recombination.

In addition to its greater stability, the *att*L complex also appears to be the dominant partner in excisive recombination. The single base change in either of the *att*L core sites decreased recombination more than the equivalent mutations in *att*R (Tables 2 to 4). Furthermore, the P ′1-C′ pair of mutants in *att*L exhibited the greatest synergism. This result, which is consistent with earlier studies (29), points to the importance of the only Int bridge that is intramolecular. Thus, as noted previously, there appears to be a functional disparity between recombination partners in excision, but it is less extreme than the disparity between *att*P and *att*B in integration (27). It is interesting that those protein binding sites capable of modulating recombination all occur on the *att*R arm: IHF inhibition of excision at H1, Xis inhibition of integration at X1X2, and Fis stimulation of excision at F (13,25,39). It seems that the primary structures of recombination are located on the *att*L arm and the modulating structures are located on the *att*R arm.

The incorporation of sequence-specific DNA bending proteins and the utilization of a bivalent DNA binding protein afford a framework for bringing two distant, or unlinked, DNA sites together. However, the intricacy of these higher order complexes cannot be entirely ascribed to the mechanistic demands of rearranging DNA since similar complexes are not observed in all site-specific recombination reactions. Even some other members of the Int family, such as Cre and FLP, that appear to use the same chemistry as λ Int for strand exchange do not exhibit this level of complexity (40). Why then the complexity? It has been suggested that higher order protein-nucleic acid complexes have evolved to meet the requirements for efficiency and precision (1). To this we would add the role of regulation, which may be an equally, if not more, important function of these complexes. We have discussed earlier how the incorporation of host-encoded proteins, such as IHF and Fis, affords a potential regulatory linkage between the recombination reactions and the physiology of the host (2,3). Other nucleic acid transactions, such as transcription regulation, DNA replication, and RNA splicing, also make use of complex higher order structures. Some of these also face the problem of accurately

bringing distant nucleic acid sites together and may make use of structural elements similar to those described for the λ recombination system.

REFERENCES AND NOTES

1. Echols H. Science 1986;233:1050. [PubMed: 2943018]
2. Landy A. Annu Rev Biochem 1989;58:913. [PubMed: 2528323]
3. Thompson, JF.; Landy, A. Mobile DNA. Berg, DE.; Howe, MM., editors. American Society for Microbiology; Washington, DC: 1989. p. 1-22.
4. Kikuchi Y, Nash HA. Proc Natl Acad Sci USA 1979;76:3760. [PubMed: 226979]
5. Craig NL, Nash HA. Cell 1983;35:795. [PubMed: 6317202]
6. Moitoso de Vargas L, Pargellis CA, Hasan NM, Bushman EW, Landy A. Cell 1988;54:923. [PubMed: 2843292]
7. Ross W, Landy A. Cell 1983;33:261. [PubMed: 6235918]
8. Ross W, Landy A. Proc Natl Acad Sci USA 1982;79:7724. [PubMed: 6218502]
9. Thompson JF, Landy A. Nucleic Acids Res 1988;16:9687. [PubMed: 2972993]
10. Craig NL, Nash HA. Cell 1984;39:707. [PubMed: 6096022]
11. Robertson CA, Nash HA. J Biol Chem 1988;263:3554. [PubMed: 2831189]
12. Yin S, Bushman W, Landy A. Proc Natl Acad Sci USA 1985;82:1040. [PubMed: 3156374]
13. Thompson JF, Moitoso de Vargas L, Koch C, Kahmann R, Landy A. Cell 1987;50:901. [PubMed: 2957063]
14. Kosturko LD, Daub E, Murialdo H. Nucleic Acids Res 1989;17:317. [PubMed: 2521383]
15. Nash HA, Robertson CA. J Biol Chem 1981;256:9246. [PubMed: 6267068]
16. Abremski K, Gottesman S. ibid 1982;257:9658.
17. Ball CA, Johnson RC. J Bacteriol 1991;173:4027. [PubMed: 1829453]
18. Moitoso de Vargas L, Kim S, Landy A. Science 1989;244:1457. [PubMed: 2544029]
19. Goodman SD, Nash HA. Nature 1989;341:251. [PubMed: 2528697]
20. Better M, Lu C, Williams RC, Echols H. Proc Natl Acad Sci USA 1982;79:5837. [PubMed: 6310548]
21. Pollock TJ, Nash HA. J Mol Biol 1983;170:1. [PubMed: 6226803]
22. Richet E, Abcarian P, Nash HA. Cell 1986;46:1011. [PubMed: 3019560]
23. Thompson, JF.; Mark, HF.; Franz, B.; Landy, A. DNA Bending and Curvature. Olson, WK.; Sarma, MH.; Sarma, RH.; Sundaralingam, M., editors. Adenine Press; Guilderland, NY: 1988. p. 119-128.
24. Thompson JF, Moitoso de Vargas L, Skinner SE, Landy A. J Mol Biol 1987;195:481. [PubMed: 2958633]
25. Moitoso de Vargas L, Landy A. Proc Natl Acad Sci USA 1991;88:588. [PubMed: 1824874]
26. Kim S, Moitoso de Vargas L, Nunes-Duby SE, Landy A. Cell 1990;63:773. [PubMed: 2146029]
27. Richet E, Abcarian P, Nash HA. ibid 1988;52:9.
28. Nunes-Duby SE, Matsumoto L, Landy A. ibid 1989;59:197.
29. Nash HA, Robertson CA. EMBO J 1989;8:3523. [PubMed: 2555168]
30. Pargellis CA, Nunes-Duby SE, Moitoso de Vargas L, Landy A. J Biol Chem 1988;263:7678. [PubMed: 2836392]
31. Bushman W, Thompson JF, Vargas L, Landy A. Science 1985;230:906. [PubMed: 2932798]
32. Numrych TE, Gumport RI, Gardner JF. Nucleic Acids Res 1990;18:3953. [PubMed: 2142765]
33. A. Landy *et al.*, unpublished results.
34. Rabbit antibody to highly purified Int (anti-Int) was used to quantify Int in each *att*R complex (26). The *att*R complexes were made with approximately 0.05 pmol of ^{32}P-labeled *att*R DNA (128 bp of Eco RI fragment) in the presence of 0.5 to 4 U of Int, 2 U of IHF, and 4 to 6 U of Xis and were fractionated by gel electrophoresis (Fig. 4). After autoradiography of the wet gel, the proteins in the complexes were transferred to an Immobilon-P membrane (Millipore), which was then incubated with anti-Int and again with peroxidase-conjugated antibody to rabbit protein. The antibody complexes were stained in the presence of H_20_2 (0.03 percent) and chloronaphthol (0.6 mg/ml). Both

the autoradiogram and the stained membrane were quantified by laser densitometry in the range of linear response. The data in each experiment were an average of the measurable complexes over the range of Int concentrations used. The ratios of band intensities on the membrane and autoradiogram were determined for each complex and were normalized to a ratio of 2 for complex RHX2. In four experiments the ratios obtained for complex RHX1 were 0.8, 0.6, 1.6, and 0.7 and for complex RHX3 they were 2.7, 3.1, 3.9, and 2.4.

35. Kikuchi Y, Nash HA. J Biol Chem 1978;253:7149. [PubMed: 359544]
36. Kotewicz M, Grzesiuk E, Courschesne W, Fischer R, Echols H. ibid 1980;255:2433.
37. K. Zahn, S. Kim, A. Landy, unpublished results.
38. Stark WM, Sherratt DJ, Boocook MR. Cell 1989;58:779. [PubMed: 2548736]
39. Thompson JF, et al. J Bacteriol 1986;168:1343. [PubMed: 2946666]
40. Argos W, et al. EMBO J 1986;5:433. [PubMed: 3011407]
41. Hsu P-L, Landy A. Nature 1984;311:721. [PubMed: 6092961]
42. S. E. Nunes-Duby and A. Landy, unpublished results.
43. The *att*L plasmid pSK1, which contains Xho I (−14) and Eco RI (+13) sites flanking the core region, and Bst BI (+48) and Nco I (+94) sites flanking the P′ arm sites, was used as the parent for *att*L mutant constructions (26). Because the pSK1 overlap region was not wild type, it was replaced either with synthetic oligonucleotides as described below or with the wild-type core region from pSN55. Mutations at the B or C′ sites were made by replacing the 28-bp Xho I-Eco RI fragment of pSK1 with synthetic oligonucleotides containing the mutated sequences. Mutations in the P′1 or P′2 sites were made by replacing the 46-bp Bst BI-Nco I fragment with synthetic oligonucleotides containing the mutated sequences. The *att*R plasmid pSN84, which contains the same Xho I-Eco RI core cassette used above, was used as the parent for all of the *att*R mutants (44). For mutations at the C and B′ sites the 28-bp Xho I-Eco RI fragment of pSN84 was replaced with the appropriate synthetic oligonucleotides. Construction and characterization of the mutant P2 site has been described (24).
44. Nunes-Duby SE, Matsumoto L, Landy A. Cell 1987;50:779. [PubMed: 3040260]
45. Excisive recombination reactions between 0.01 pmol of ^{32}P-labeled linear *att*L and 0.1 pmol of supercoiled *att*R DNA were performed at 25°C in 20 μl of tris-HCl (pH 7.4), 60 mM NaCl, 2 mM dithiothreitol, 5 mM EDTA, 6 mM spermidine and bovine serum albumin (BSA) (100 μg/ml) in the presence of 1 U of Int, 1 U of IHF, and 2 U of Xis for 6 hours. For the reactions in Table 2, 6 U of Xis were used; in Table 4, the NaCl concentration was 50 mM. The reaction mixtures were subjected to electrophoresis in 1.2 percent agarose and autoradiograms were quantified with an LKB Ultra-scan densitometer.
46. Landy A, Ross W. Science 1977;197:1147. [PubMed: 331474]
47. Winoto A, Chung S, Abraham J, Echols H. J Mol Biol 1986;192:677. [PubMed: 3031315]
48. Gardner JF, Nash HA. ibid 1986;191:181.
49. The nicked substrates top or bottom strand (5′ end-labeled) were made from the 908-bp Apa Li-Sal I fragments of pSN82 or pSN92 (42). The half-*att*R was prepared by 5′ end-labeling the 114-bp Eco RI-Xba I fragment of pSN82 (26). All of these *att*R fragments are H1^{-} mutants to prevent IHF inhibition of excisive recombination (39). Approximately 0.01 pmol of ^{32}P-labeled suicide substrates were mixed with 0.5 U of Int in the presence or absence of 1 U of IHF and 2 U of Xis under the recombination conditions described above, but at 120 mM NaCl. (The IHF and Xis dependence is best seen under conditions of limiting Int.) The reactions also contained 0.1 pmol of *att*L or pBR322 DNA. The reactions were terminated after 4 hours with 0.1 percent SDS and analyzed by gel electrophoresis: reactions with nicked substrates, on 1.8 percent agarose gels containing 0.1 percent SDS; cleavage reactions with the half-*att*R, on 5 percent polyacrylamide containing 0.1 percent SDS; and recombination (top-strand transfer) reactions of the half-*att*R, on 1.2 percent agarose-2 percent polyacrylamide composite gels. The gels were dried, autoradiographed, and quantified by densitometry.
50. The 128-bp Eco RI *att*R fragment was obtained from pSN82, gel-purified, and 5′ end-labeled with ^{32}P. Approximately 0.01 pmol of ^{32}P-labeled DNA was incubated with 1 U of IHF and 2 U of Xis at 25°C in 20 μl of 10 mM tris-HCl (pH 7.5), 50 mM NaCl, 1 mM EDTA, BSA (1 mg/ml), and salmon sperm DNA (100 μg/ml). Int (0.06 to 2 U) was added and after a 5-minute incubation at 25°

C, the mixtures were analyzed on 5 percent polyacrylamide gels and the products were quantified by densitometry of the autoradiograms.

51. We thank members of our laboratory for helpful discussions; S. Nunes-Duby and J. Boyles for preparation of the manuscript; T. Oliveira for technical assistance; D. Brautigan for advice on immunoblotting; and F. Stahl for suggestions about the manuscript. Supported by NIH grants Al 13544 and GM 33928.

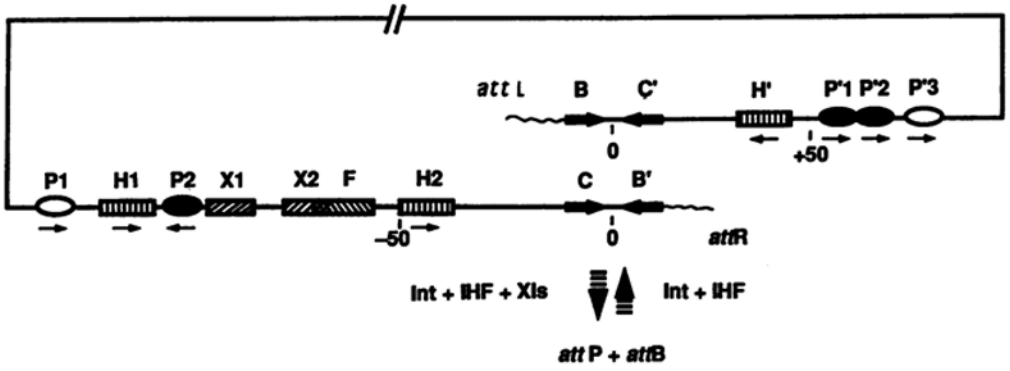

Fig 1.

Protein binding sites in *att*L and *att*R. The *att*L and *att*R sites are separated by 40,000 bp and comprise the junctions between phage DNA (straight line) and bacterial DNA (wavy lines). Nucleotide 0 is placed within the 7-bp overlap region, and the coordinates have positive numbers to the right and negative numbers to the left (46). The arm-type sites (ovals), bound by the NH_2-terminal domain of Int, are labeled P1 and P2 in *att*R and P′1, P′2, and P′3 in *att*L. The core-type sites (large arrows), bound by the COOH-terminal domain of Int, are labeled C and B′ in *att*R and B and C′ in *att*L. Those Int binding sites required for excisive recombination are denoted by solid ovals and arrows; unfilled ovals denote arm-type Int sites used only for integrative recombination (24,32,47). Binding sites for the DNA bending proteins are indicated by rectangles: the IHF binding sites (vertical lines) are H′ in *att*L and H1 and H2 in *att*R, the H1 site is used only for integrative recombination and its occupancy by IHF inhibits excisive recombination (39,48); the Xis binding sites (rising slashes) are X1 and X2; the Fis binding site, F (falling slashes), overlaps the X2 site. Int binding at P2 is promoted by cooperative interactions with Xis at X1X2 (12,24). The relative orientations of the DNA binding sites are indicated by arrows.

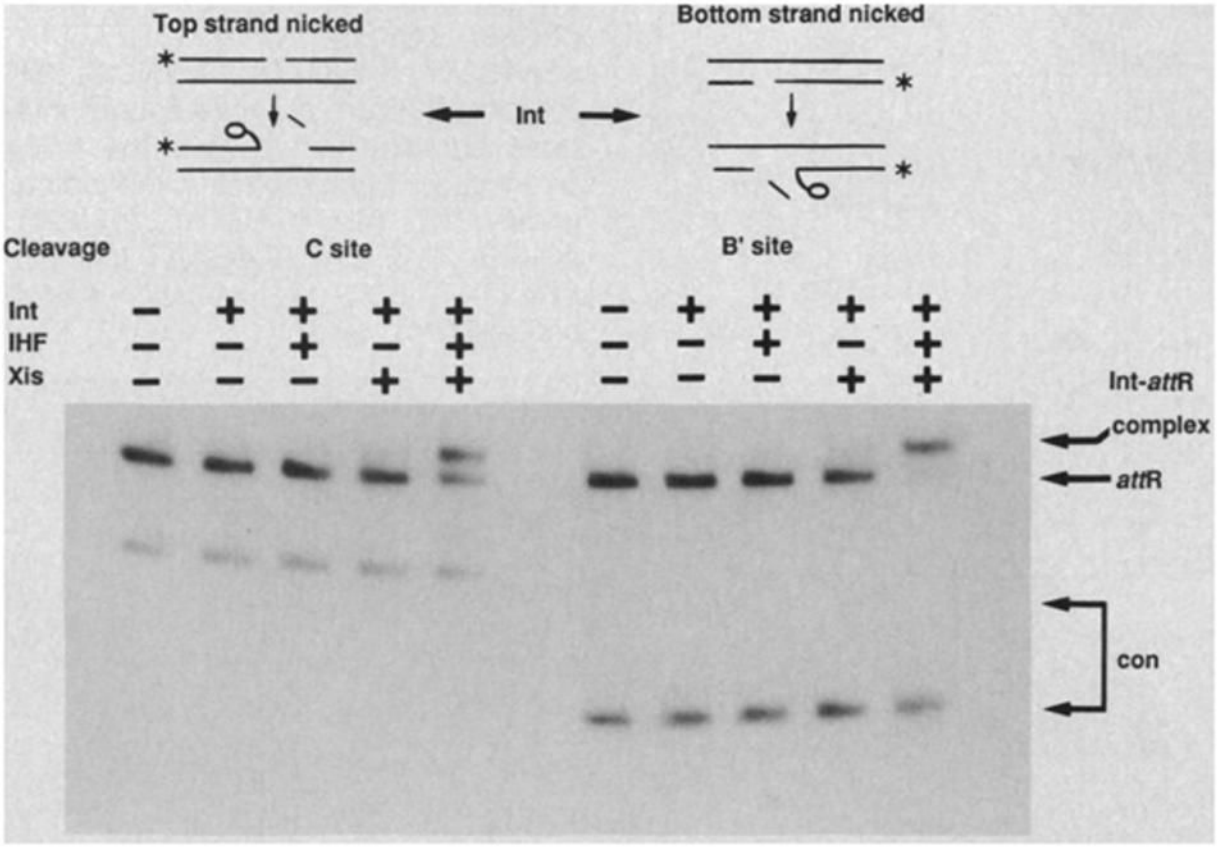

Fig 2.

IHF and Xis dependence of Int cleavage at the core sites of *att*R. (Top) Diagram of how the *att*R suicide substrates lead to formation of covalent Int-DNA complexes after Int cleavage at the C core site (top-strand nicked substrate) or at the B′ core site (bottom-strand nicked substrate). The 5′ terminus of the nicked strand was labeled with ^{32}P (49). (Bottom) Gel electrophoresis of the reactions of top- or bottom-strand nicked suicide substrate in the presence (+) or absence (−) of indicated proteins (49). The gel mobility of covalent complex (Int-*att*R) and *att*R suicide substrates is shown in the right margin. DNA fragments generated during the preparation of the suicide substrates are indicated as con.

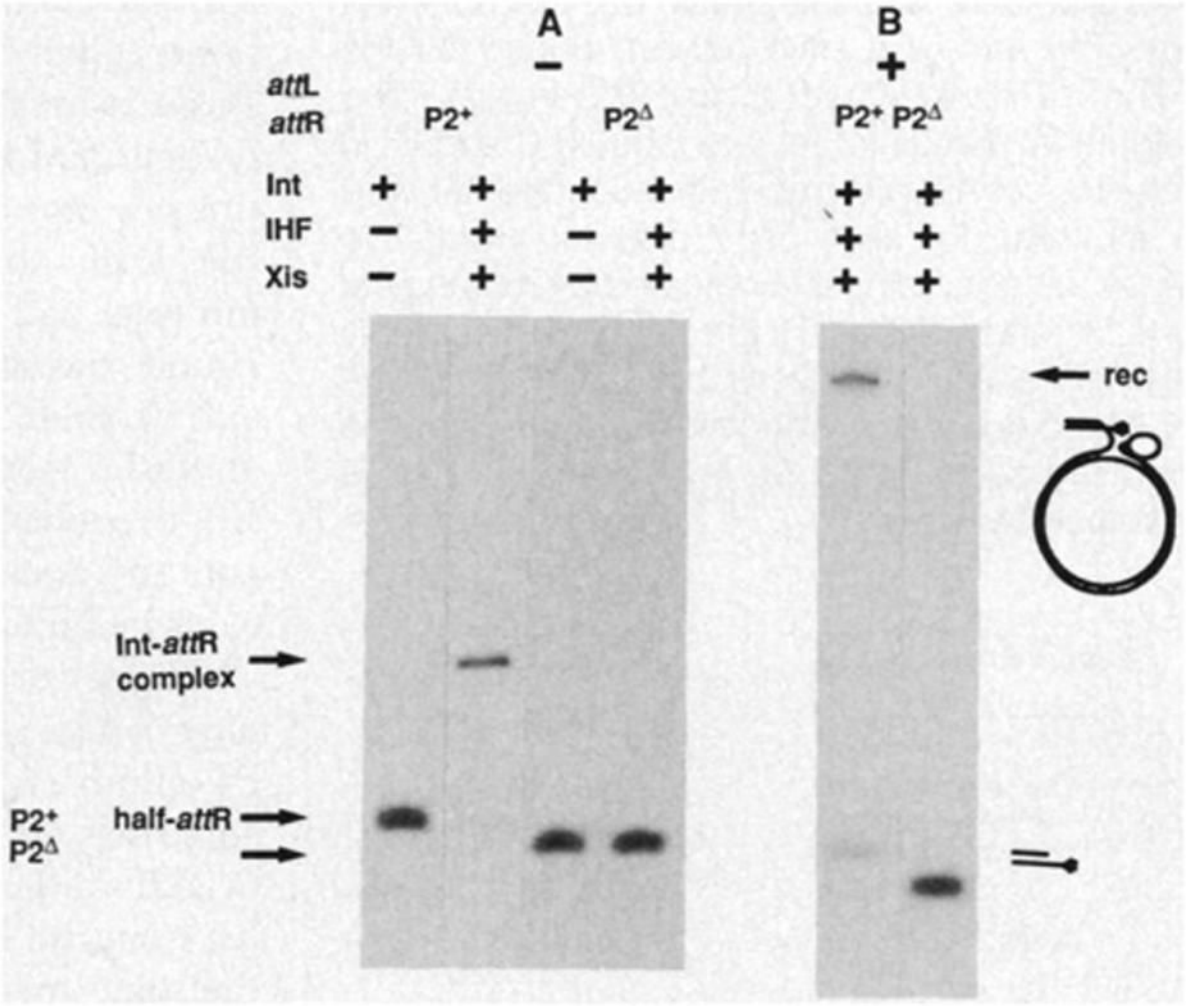

Fig 3.

P2 dependence of Int cleavage and top-strand transfer. (**A**) Gel electrophoresis of covalent Int-DNA complexes at the C site of a half-*att*R with a wild-type ($P2^+$) or P2-deleted (P2Δ) arm-type site, in the presence (+), or absence (−), of indicated proteins (49). The mobilities of the half-*att*R and Int-DNA complexes are indicated in the left margin. (**B**) Gel electrophoresis of a top-strand transfer assay for the $P2^+$, or the P2-deleted, half-*att*R (^{32}P-labeled) with wild-type *att*L. The product of top-strand transfer is indicated in the right margin (rec) and its structure is shown (28). These reactions contain 0.1 pmol of *at* L DMA instead of the pBR322 carrier DMA (49).

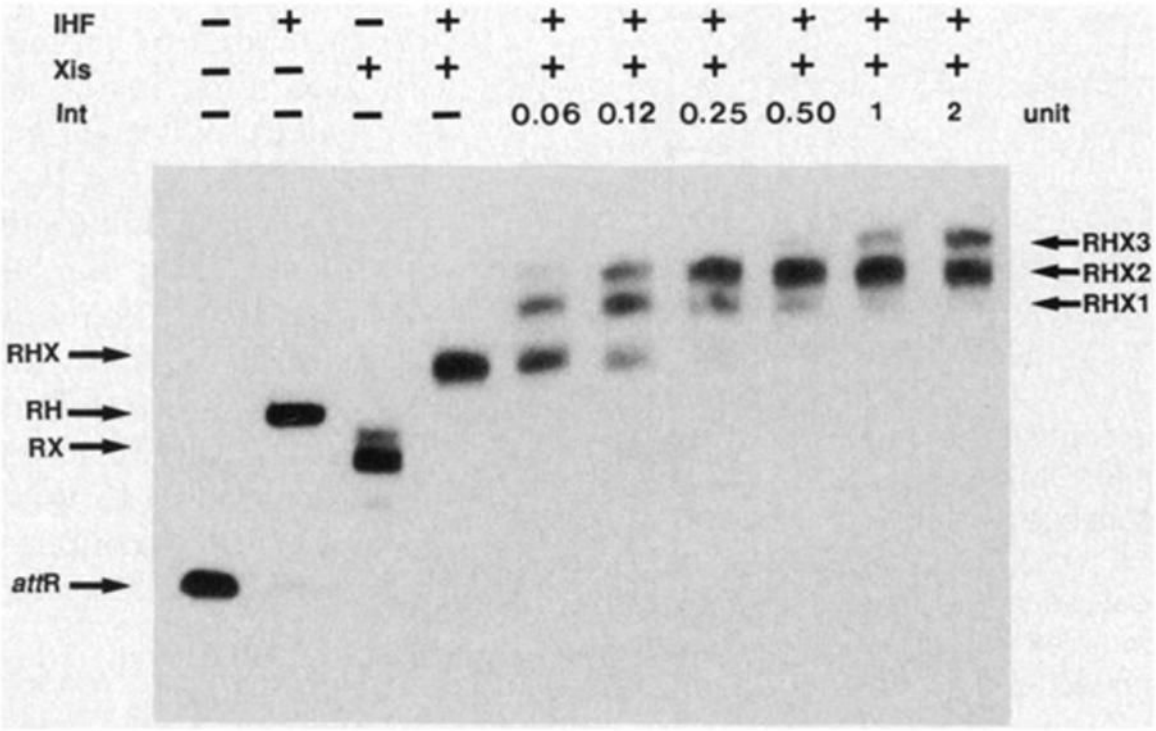

Fig 4.

Gel retardation of *att*R higher order complexes. An *att*R (extending from the P2 site to the B′ core site) was incubated with the indicated proteins to generate complexes containing IHF (RH), Xis (RX), and IHF plus Xis (RHX). Complexes RHX1–RHX3 were generated by the addition of the indicated amounts of Int to complex RHX (50).

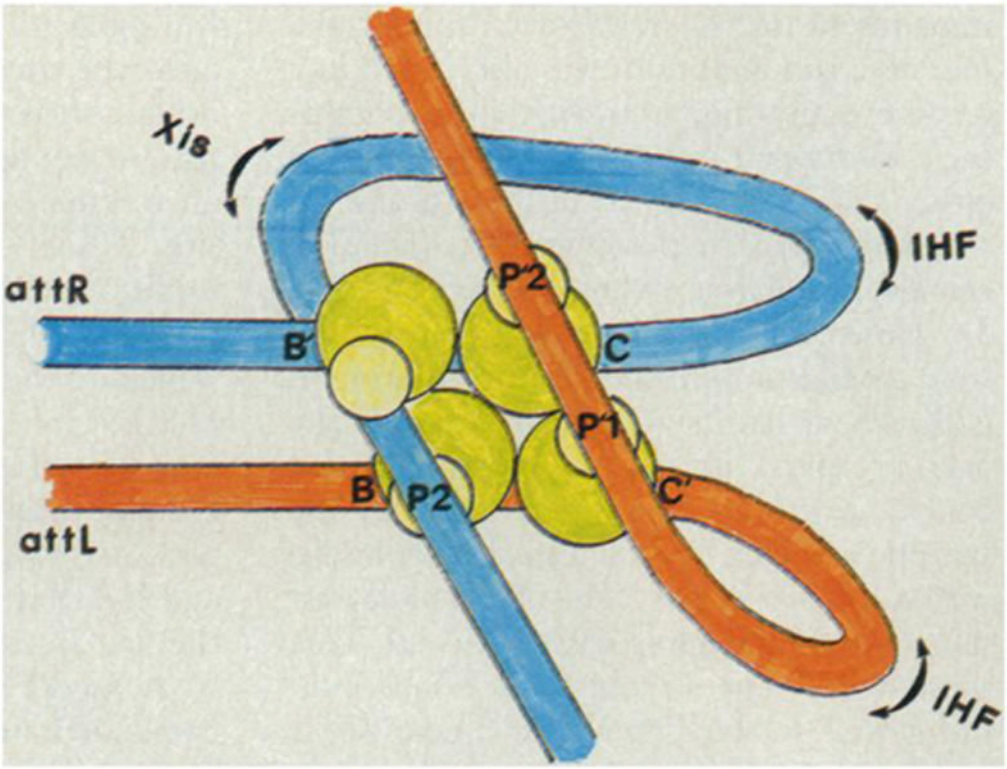

Fig 5.

A model for the Int-mediated synaptic interactions between the arm and core sites of *att*L and *att*R during excisive recombination. Bends in the *att*R (blue) and *att*L (orange) DMA are induced by IHF and Xis. The bivalent Int protein (green) forms intra-and intermolecular bridges: binding to the high-affinity arm sites (P′1, P′2, and P2) is via the smaller NH_2-terminal domain (small circle) and binding to the low-affinity core sites (B, B′, C, and C′) is via the larger COOH-terminal domain (large circle), which also contains the topoisomerase function. The relative positions of proteins and DMA in space and the relative order of interactions in time are not in the model.

Table 1

Mutants of *att*L and *att* R used for the pairwise test for synergism. Mutant core sites are indicated as underlined lowercase letters and mutant arm sites are denoted by a superscript minus. Wild-type (WT) *att*R was from pPH202 (41). Wild-type *att*L was from pSN55, which was derived from pPH201 (41) by introducing an Eco RI site at +13 and filling in the Eco RI site of pBR327 (42). Base substitution mutants in the core- and arm-type Int binding sites were constructed with synthetic oligonucleotides that were inserted into the appropriate plasmids (43). All of the core mutants contained a C substitution at the third position of the consensus recognition sequence to give the following for each mutant core site in the indicated plasmids: B, CTCCTTTTT (pSK4, pSK22, pSK25); C′, CACCTTAGT (pSK9, pSK23, pSK26); C, CACCTTTTT (pSK13, pSK15); B′, CACGTTAGT (pSK14, pSK16). The P′1 and P′2 arm mutants each contained two base substitutions to give the following sequences for each mutant in the indicated plasmids: P′1, AGCTCAGTAT (pSK24, pSK25, pSK26); P′2, CACTCAGAAT (pSK21, pSK22, PSK23). The P2 arm mutation has been described (24).

Arm	Core	Plasmid
*att*L		
WT	WT	pSN55*
WT	bOC′	pSK4
WT	BOc′	pSK9
P′2$^-$	WT	pSK21
P′ 2$^-$	bOC′	pSK22
P′ 2$^-$	BOc′	pSK23
P′ 1$^-$	WT	pSK24
P′ 1$^-$	bOC′	pSK25
P′ 1$^-$	BOc′	pSK26
*att*R		
WT	WT	pPH202†
WT	cOB′	pSK13
WT	COb′	pSKU
P2$^-$	WT	pJT33‡
P2$^-$	cOB′	pSK15
P2$^-$	COb′	pSK16

*(42).

†(41).

‡(24).

Table 2

Pairwise test for synergism between a mutant P2 (arm-type) Int binding site and each of the four mutant core-type Int binding sites. In each recombination reaction, one, or none, of the four core sites (B, B′, C, and C′) is mutant (designated by an underlined lowercase letter). A wild-type core is designated WT. The mutant core site is either in the *att*L or *att*R partner. For each configuration of core sites there are two recombination reactions: in one the *att*R has a wild-type ($P2^+$) arm site, in the other it has a mutated ($P2^-$) arm site (Table 1). The recombination with each *att*R partner ($P2^+$ and $P2^-$) has been normalized to 100 percent for the reaction with all wild-type sites (the absolute level of recombination for the wild-type reaction was greater than 70 percent) (45).

Core		Percent recombination		
***att*L**	***att*R**	**$P2^+$**	**$P2^-$**	**Ratio ($P2^-/P2^+$)**
WT	WT	100	77	0.77
b̲OC′	WT	33	5	0.15
BOc̲′	WT	22	9	0.41
WT	c̲OB′	70	83	1.19
WT	COb̲′	69	66	0.96

Table 3

Pairwise test for synergism between a mutant P′2 (arm-type) Int binding site and each of the four mutant core-type Int binding sites. The core sites are identical to those in Table 2. For each configuration of core sites there are two recombination reactions: in one, the *att*L partner has a wild-type (P′2^{+}) arm site, and in the other it has a mutated (P′2^{-}) arm site. See also the Table 2 legend.

Core		Percent recombination		
***att*L**	***att*R**	**P′2^{+}**	**P′2^{-}**	**Ratio P′2^{-}/P′2^{+}**
WT	WT	100	84	0.84
b̲OC′	WT	16	16	1.00
BOc̲′	WT	26	30	1.15
WT	c̲OB′	49	23	0.47
WT	COb̲′	65	28	0.43

Table 4

Pairwise test for synergism between a mutant P′1 (arm-type) Int binding site and each of the four mutant core-type Int binding sites. The core sites are identical to those described in Table 2. For each configuration of core sites there are two recombination reactions: in one the *att*L partner has a wild-type ($P'1^+$) arm site, and in the other it has a mutated ($P'1^-$) arm site. See also the Table 2 legend.

Core		Percent recombination		
***att*L**	***att*R**	**$P'1^+$**	**$P'1^-$**	**Ratio $P'1^-/P'1^+$**
WT	WT	100	63	0.63
b̲OC′	WT	79	11	0.14
BOc̲′	WT	81	1	0.01
WT	c̲OB′	82	46	0.56
WT	COb̲′	109	67	0.61